

# OBSERVATION AND PREDICTION OF LOCAL DAMAGE PATTERNS UNDER TENSION AND TORSION HIGH CYCLE FATIGUE

L. FLACELIERE<sup>1</sup>, F. MOREL<sup>1</sup> and A. DRAGON<sup>1</sup>

<sup>1</sup>Laboratoire de Mécanique et de Physique des Matériaux (UMR CNRS 6617), Ecole Nationale Supérieure de Mécanique et d'Aérotechnique, 86961 Futuroscope Chasseneuil Cedex, France

## ABSTRACT

This paper aims at comparing the experimental fatigue strength of samples loaded in high cycle fatigue (HCF) and the predictions employing a damage model dedicated to the HCF. The material studied, a mild steel C36, is tested for lifetime ranging from  $10^5$  to  $10^6$  cycles. Some observations (by SEM) are carried out during the tests performed under fully reversed tension ( $R=-1$ ) or under fully reversed torsion ( $R=-1$ ).

The proposed model considers the material behaviour at a local mesoscopic scale and makes appear a coupling between plasticity due to gliding in shear bands and damage occurring when the accumulated plastic strain at the grain scale has reached a threshold value. The irreversible thermodynamics with internal state variables is employed to keep a middle way between extensive description of plastic flow and damage and application accessibility requirements.

After identification of the model parameters by using tension and torsion Wöhler curves, it is shown that the model is able to reflect both the fatigue limit mechanisms through the concept of elastic shakedown and the microcrack growth, considered as a local damage evolution. The observations under tension and torsion are in good agreement with the model predictions especially when the crack size is of the same order as the microstructure characteristic length.

## 1 INTRODUCTION

The most classical approach in damage mechanics is the effective stress concept, introduced by Kachanov to describe creep under unidimensional stress [1]. Later, Chaboche [2] has proposed a phenomenological model using a scalar damage variable able to deal with creep, High and Low Cycle Fatigue. In the HCF regime, this model presents the possibility of damage evolution below the fatigue limit (after damage initiation).

In HCF, for the most part, there is no noticeable macroscopic plasticity; localized micro-plasticity is the main cause of shear band nucleation and crack initiation. Damage can then be considered as a process of progressive deterioration of the grain less favourably oriented to the external loading (irreversibility). So, damage acting like a degradation of the material cohesion. To reflect this damage feature, Lemaître and al. proposed to use a scalar damage variable, and assume that the HCF damage takes place on a lower scale than the macroscopic scale [3]. More exactly, a spherical inclusion loaded in the elastic-plastic regime (with damage) is embedded into a macroscopic (infinite) elastic or elasto-plastic matrix. At the inclusion scale, the redistribution stress effect due to the damage evolution acts through the effective stress. However in HCF, damage mechanisms are different from those occurring in creep, and physical justifications of the use of the effective stress concept may be questionable.

Few other damage models are applied or dedicated to HCF. For instance, Abdul-Latif and Saanouni consider three scales (macroscopic, grain scale, and crystallographic glide systems), with different localization and homogenisation operations [4]. Seweryn and Mroz built a specific damage-and-failure model for the physical plane element to deal with HCF, without explicit consideration of local plasticity [5].

In this study, the use of an intermediate way between phenomenological approach and complex description on many scales is made. The proposed model considers material evolution at the mesoscopic scale, in particular local plasticity, and is based on a simple micro mechanical approach, where plasticity and damage are defined and coupled at the grain scale. To reach the stress and strain fields at this scale, different rules can be introduced (Lin-Taylor, self consistent scheme, ...). For sake of simplicity, the Lin-Taylor proposal (1) is utilized :

$$\underline{\underline{\sigma}} = \underline{\underline{\Sigma}} - 2\mu\underline{\underline{\varepsilon}}^p \quad (1)$$

where  $\underline{\underline{\sigma}}$  and  $\underline{\underline{\varepsilon}}^p$  represent the stress and plastic strain tensors at the mesoscopic scale and  $\underline{\underline{\Sigma}}$  is the macroscopic stress tensor.

## 2 EXPERIMENTAL RESULTS AND OBSERVATIONS IN TENSION AND TORSION

The material studied is a mild steel C36 composed of grains of ferrite and grains of pearlite. The chemical composition of this steel is given in Table 1 while the mechanical characteristics are shown in Table 2.

Fe	C	Si	Mn	S	P	Ni	Cr	Co	Mo	W	V	Ti
98,4	0,36	0,27	0,6	0,009	0,034	0,07	0,14	0,07	0,01	0,01	0,005	0,009

Table 1. Chemical composition of the C36 steel in average weight (%)

Young modulus	R <sub>P 0,2</sub> <i>monotonous</i>	R <sub>P 0,2</sub> <i>cyclic</i>	R <sub>m</sub>	A%
205000MPa	350MPa	280MPa	580MPa	30%

Table 2. Mechanical characteristics of the C36 steel

In order to reduce the scatter of the test results, mechanical polishing was performed with several abrasive papers up to a grain size of 6µm. Finally, the polishing procedure ends with a paste diamond of one micron. Before fatigue tests and in order to remove the residual stresses occurring during the specimen preparation, all the samples underwent a tempering at 500°C during one hour under vacuum. The whole experimental work was conducted at room temperature and under air environment on a servohydraulic biaxial testing machine (Instron type 1343) operating in force (and torque) control in the frequency range 10-20 Hz.

Once the specimen fails, a replica technique using a bi-component dental resin and applied at the specimen surface on the gauge length, indicates evolutions of each individual crack. After metallization, some observations on a SEM (under low acceleration voltage, in order to preserve the conducting film). This technique was first tested by Palin-Luc from LAMEFIP in Bordeaux.

On all observed specimens in tension (7 samples), the importance of the two critical planes related either to the maximum shear stress or to the maximum principal stress appears as evidence. The plane of maximum shear stress corresponding to the first stages of nucleation and the beginning of short crack growth (stage I, mode II) are represented by dark full lines in Figure 1. After this first phase of shear crack growth, the crack branches toward a plane of maximum normal stress (stage II, mode I) represented by white dashed lines in Figure 2. This branching occurs for a maximum crack length of 20µm. According to the observation carried out on all the specimen surface, it occurs that the damage is very localized. Very few signs of damage or plasticity on the gauge length are observed. All the tension cracks initiated on a surface defect (due to polishing), on an inclusion (sulphide) or on plastic shear bands occurring on the sample surface.

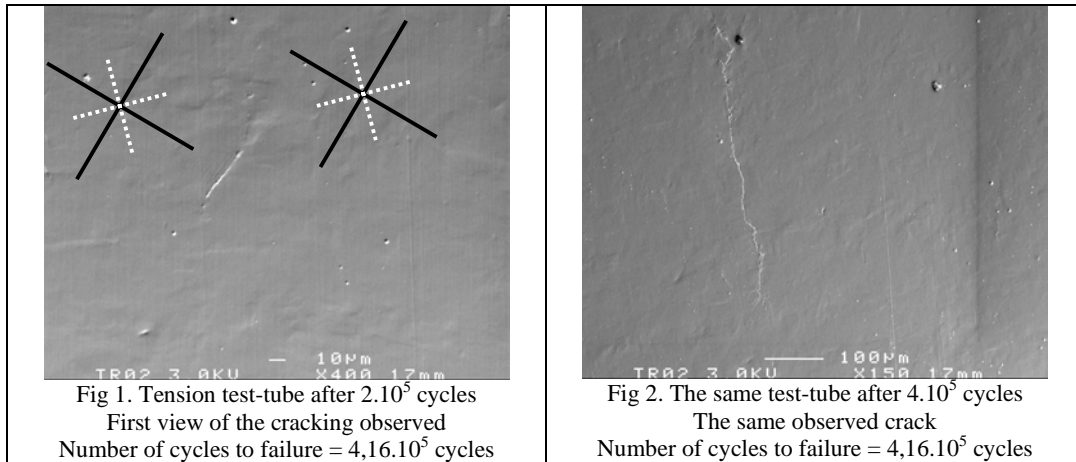


Figure 3 shows the crack length in function of the applied number of cycles for the four principal cracks observed all along the test time. It appears clearly that the cracks n° 1 and 2 start to grow after their initiation but stop their propagations because they meet a microstructural barrier such as the pearlite bands. Two other cracks n° 3 and 4 show an increase of the crack speed with the applied number of cycles but only one crack (n°4) leads to failure. This observation proves the high degree of damage localisation in this fatigue life regime and shows that microdamage sites can exhibit growth independently of each other, i.e. grow without interactions.

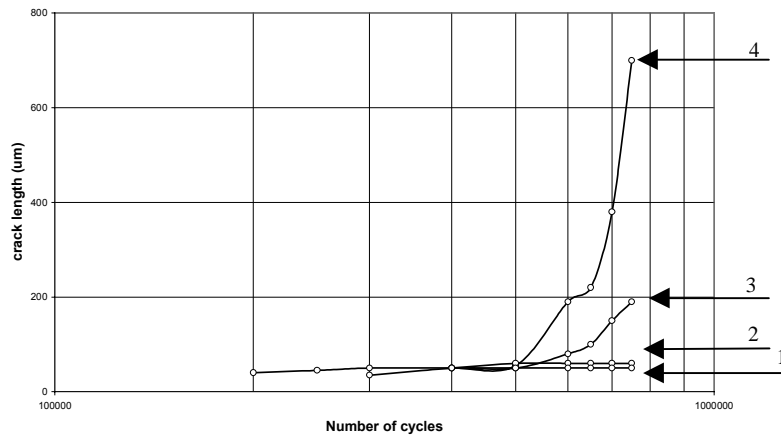


Fig 3. Crack length in function of number of applied cycles for four cracks occurring on the specimen C36TR06 submitted to tension

Under fully reversed torsion loading mode, the observations show that the first stages of crack initiation are governed by mode II along the planes of maximum shear stress. These planes correspond to the longitudinal and transverse directions to the specimen axis. On a specimen showing a number of cycles to failure of  $4 \cdot 10^5$ , one can already distinguish after only  $10^5$  cycles (for several tests) many cracks and plastic shear bands oriented along these two directions, with a length of about  $20 \mu\text{m}$  and an almost homogeneous distribution on the specimen gauge length. During the following cycles, new cracks can develop but the already existing cracks keep growing mainly along the longitudinal axis. In the case of the specimen in Figure 4, the first crack coalescence are observed after  $5 \cdot 10^5$  cycles, around the half the sample lifetime. The failure occurs after the shear crack branches to  $45^\circ$  along the plane of maximum normal stress. Figure 5 shows such a crack where the stages I and II are clearly distinguished.

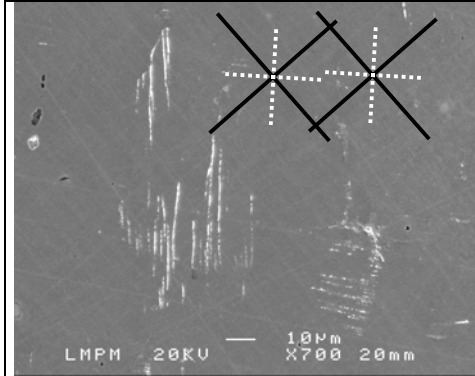


Fig 4. A torsion test-tube after  $10^5$  cycles  
Accumulative plastic strain on critical mode II plans  
Number of cycles to failure =  $4.10^5$  cycles

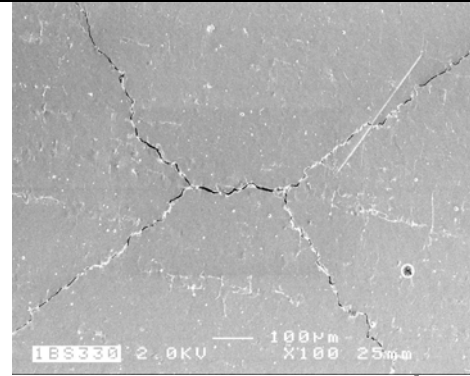


Fig 5. An other torsion test-tube after  $8.10^5$  cycles  
It is near the end of the life of the sample  
Number of cycles to failure =  $9.10^5$  cycles

According to these observations conducted on five specimens, it is important to point out the very different damage mechanisms under torsion and tension. The tension loading leads to very few cracks while the damage pattern due to torsion is more homogeneous on the specimen surface. The damage kinetics is different, and the damage modelling must correctly reflect this feature.

### 3 MESOSCALE DAMAGE MODEL FOR HCF

The framework of the irreversible thermodynamics with internal variables for time-independent, isothermal transformations and small deformations is used. The model summarised below allows the existence of a state potential, the free energy, as well as the existence of a dissipation potentials involving distinct multipliers, a normal dissipation being thus assumed for each mechanism (plasticity, damage). The axiom of the local accompanying state (LAS) induces a description of the continuous medium at a given point and at a given time, according to the knowledge (at this place and at this time), of a few state variables [6]. The choice of uncoupled dissipations for plasticity and damage [7] makes easier the distinction of the associated mechanisms and the two criteria. This choice leads, in particular, to account for local plastic straining before any damage development.

The elastic and inelastic parts of the granular specific free energy are written as follows :

$$\omega = \rho\psi = \omega^e(\underline{\underline{\varepsilon}}^e) + \omega^p(\underline{\underline{\varepsilon}}^p, p, d) + \omega^d(d, \beta) \quad (2)$$

$$\text{or } \omega = \frac{1}{2}(\underline{\underline{\varepsilon}} - \underline{\underline{\varepsilon}}^p) : \underline{\underline{C}} : (\underline{\underline{\varepsilon}} - \underline{\underline{\varepsilon}}^p) + \frac{1}{2}c\underline{\underline{\alpha}} : \underline{\underline{\alpha}} + \tilde{r}_\infty p \exp(-sd) + \frac{\tilde{r}_\infty}{g} \exp(-gp) \exp(-sd) + F_{d0}d + \frac{1}{2}q\beta^2 \quad (3)$$

$$\text{The intrinsic dissipation, at the grain level is given by (4) : } \Phi = \underline{\underline{\sigma}} : \underline{\underline{\dot{\varepsilon}}}^p - \underline{\underline{x}} : \underline{\underline{\dot{\alpha}}} - r \cdot \dot{p} + F_d \dot{d} - k\dot{\beta} \geq 0 \quad (4)$$

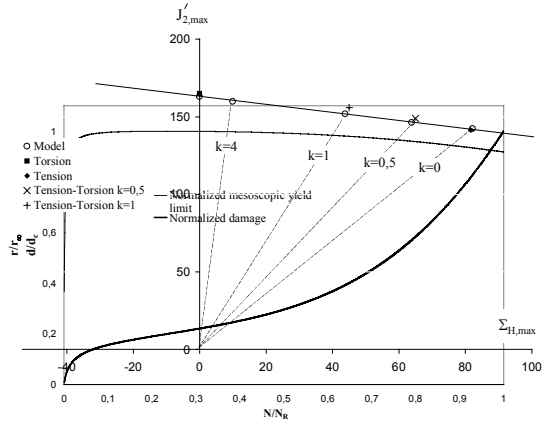
$$\text{The plastic load surface at the mesoscopic scale is defined as : } f(\underline{\underline{\sigma}}, \underline{\underline{x}}, r) = J_2(\underline{\underline{\sigma}} - \underline{\underline{x}}) - (r + r_0) \leq 0 \quad (5)$$

$$\text{Where } J_2'(\underline{\underline{\sigma}} - \underline{\underline{x}}) = \sqrt{\frac{1}{2}(\underline{\underline{s}} - \underline{\underline{x}}) : (\underline{\underline{s}} - \underline{\underline{x}})} \quad (6) \quad \underline{\underline{s}} = \underline{\underline{\sigma}} - \frac{1}{3}Tr(\underline{\underline{\sigma}}) \quad (7) \quad \underline{\underline{x}} = \frac{\partial \omega}{\partial \underline{\underline{\alpha}}} = c\underline{\underline{\alpha}} = c\underline{\underline{\varepsilon}}^p \quad (8)$$

The specific form of  $J_2'$  equals the applied shear stress for a pure shear loading. The kinematic hardening is based on the model proposed by Prager [7]. The thermodynamic force representing the isotropic hardening threshold is given by (9), with  $g$  hardening related constant and  $s$  damage sensitivity one.

$$r = \frac{\partial \omega}{\partial p} = r_\infty (1 - \exp(-gp)) \exp(-sd) \quad (9)$$

The latter equation defines the coupling between plasticity and damage. Figure 6 shows the evolution of the yield stress  $r$  with the number of cycles applied for a pure torsion loading. As damage increases, the isotropic



hardening is lowered. In the same time, the kinematic hardening, that is not affected by damage, remains active. The isotropic part of the hardening tends then to vanish and an elastic shakedown state is impossible to reach. The initiation and the subsequent failure of the component is then likely to occur due to the exhaustion of the ductility.  $F_d$  is the thermodynamic force associated to the damage variable  $d$ . This force depends both on the accumulated plastic strain  $p$  and the damage  $d$ .

<p>Fig 6. Normalized elastic domain (<math>r/r_\infty</math>) and normalized damage (<math>d/d_c</math>) in function of the number of cycles in torsion (165 MPa)</p>	<p>Fig.7 Predicted threshold endurance curve (at <math>10^6</math> cycles and for a 50% failure probability) and experimental data in the plane (<math>J'_{2,max}, \Sigma_{H,max}</math>)</p>
---	---

A nonassociated law is used for the damage evolution (distinction between the damage locus and the damage potential). Equation (10) gives the damage load function, where  $a$  is the hydrostatic stress sensitivity coefficient relative to the damage threshold, and  $k_0$  the initial damage threshold. In other words,  $k$  governs the damage threshold evolution while the damage potential (11) shows a similar form but exhibits a different hydrostatic stress sensitivity parameter  $b$  for the damage development.

$$h(F_d, k; \sigma_h) = F_d (1 + a \sigma_h) - (k + k_0) \quad (10)$$

$$H(F_d, k; \sigma_h) = F_d (1 + b \sigma_h) - (k + k_0); \quad \dot{d} = \lambda^d \frac{\partial H}{\partial F_d} \text{ avec } \lambda^d \geq 0 \quad (11)$$

$$F_d = -\frac{\partial \omega}{\partial d} = \tilde{r}_\infty s \exp(-sd) \left( p + \frac{\exp(-gp)}{g} \right) + F_{d0} \quad (12)$$

A second scalar variable, denoted as  $\beta$ , is defined as the cumulated damage measure. Its conjugate force is denoted as  $k$  and depends linearly on  $\beta$ . This form of modelling is close to the Murakami proposal [8].

$$k = -\frac{\partial \omega}{\partial \beta} = q\beta \quad (13)$$

Application of this model as a predictive tool to the tests non-employed for the model identification leads to a fair good predictively for proportionnal tension-torsion loading paths, see Figure 7.

#### 4 DISCUSSION AND CONCLUSION

Some tests carried out on a mild steel are conducted to compare the local damage evolution under tension and torsion loading. For fatigue lives related to stress levels just above the fatigue limit, it appears that the tension and the torsion cracks initiate and grow first according to a shear mode (stage I, mode II) and then branch to a

normal mode (stage II, mode I). However the damage patterns are very different under torsion and tension. While very few tension cracks initiate and grow, the plastic shear bands and the cracks under torsion are observed everywhere on the specimen surface, for stage I mostly along the specimen axis, i.e. along the pearlite bands.

The framework of the irreversible thermodynamics processes with internal variables is used to build a damage model that can reflect these damage features. The local plasticity playing a fundamental role in this fatigue regime, simple mesoscopic cyclic hardening rules are employed. The model leads to the prediction of the fatigue limit (defined as the stress limit under which no initiation occurs) according to the concept of elastic shakedown. So, this modelling remains more adapted for nucleation and the propagation of crack in mode II, for which the lips of the cracks are rubbing, and leads to accumulation of the plastic strain. Moreover, with this approach, the damage nucleation and its growth are governed by different laws. The effect of the hydrostatic stress on the threshold is different from its influence on the damage evolution. This property is interesting and to our knowledge none of the existing models could deal efficiently with this problem.

Moreover, coupling with a probabilistic approach will have to be developed, to account for the strong dispersion of the kinetics of propagation of fatigue cracks. In the future, it will made projection of the of the stress tensors components and plastic deformations in a physical plane particular directions given will make it possible to obtain an approach by critical direction.

1. KACHANOV, L.M., *Time of the rupture process under creep conditions*. *Isv. Akad. Nauk., Otd Tekh. Nauk.*, 1958. **8**: p. 26-31.
2. CHABOCHE, J.L., *Une loi différentielle d'endommagement de fatigue avec cumulation non-linéaire*. *Rev. Fr. Méc.*, 1974. **50-51**: p. 71-82.
3. LEMAITRE, J., J.P. SERMAGE, and R. DESMORAT, *A two scale damage concept applied to fatigue*. *International Journal of Fracture*, 1999: p. 67-81.
4. ABDUL-LATIF, A. and K. SAANOUNI, *Damaged anelastic behaviour of FCC polycrystalline metals with micromechanical approach*. *International Journal of Damage mechanics*, 1994. **3**: p. 237-259.
5. SEWERYN, A. and Z. MROZ, *On the criterion of damage evolution for variable multiaxial stress states*. *Solids Structures*, 1997. **35**(14): p. 1586-1616.
6. BATAILLE, J. and J. KESTIN, *L'interprétation physique de la thermodynamique rationnelle*. *Journal de Mécanique*, 1975. **14**(2): p. 365-384.
7. PRAGER, W., *Non Isothermal Plastic Deformation*. Koninklijke Nederlandse Akademie van Wetenschappen, 1958. **61**: p. 176-182.
8. MURAKAMI, S. and K. KAMIYA, *Constitutive and damage evolution equations of elastic-brittle materials based on irreversible thermodynamics*. *Int. J. Mech.Sci.*, 1997. **39**(4): p. 473-486.